JOURNAL OF MATERIALS SCIENCE 12 (1977) 503–508

The fracture behaviour of ABS polymers

R. W. TRUSS, G. A. CHADWICK
Department of Mining and Metallurgical Engineering, University of Queensland, St. Lucia, Queensland 4067, Australia

The fracture behaviour of three different grades of ABS has been investigated over a range of temperature and strain-rates. A two-stage fracture process has been observed consisting of a slow crack propagation region followed by catastrophic failure. The surface features in these two regions have been examined in detail using scanning electron microscopy. In all cases, the fracture initiation site was located at either a surface defect or at an internal inclusion much larger than the average rubber particle size.

1. Introduction

In our previous work, we reported briefly on the fracture of a transparent ABS [1]. We observed a transition on the fracture surface from a highly drawn fibrilar structure in the slow crack growth region to a more irregular surface in the catastrophic crack growth region. We also reported cracks initiating in large distinct crazes at a strain-rate of 1.4×10^{-4} sec^{-1} and in highly stress whitened regions at a strain-rate of 1.4×10^{-1} sec^{-1}.

This present work was undertaken to systematically study the fracture of ABS polymers. Specimens of three grades of pigmented ABS with different volume fractions of elastomer phase were tested to assess the effect of rubber content on the fracture behaviour. Strain-rate and temperature were also varied since previous work on pigmented ABS indicated that these parameters affect the crazing behaviour [2].

2. Experimental

2.1. Materials

The materials used were various grades of Cycolac brand commercial ABS with constant matrix molecular weight but varying rubber content. Three different rubber content materials were tested in the present series of experiments and these were designated as shown in Table 1. The rubber particles had a range of sizes between 0.05 and 1 μm with the average particle size being 0.3 μm.

TABLE I Designation of material used

Rubber content	Designation
Low, 15 wt%	A
Medium, 20 wt%	B
High, 30 wt%	C

Specimens for room temperature tests were injection-moulded to a shape specified by BS2782 having a parallel gauge length of 50.8 mm with a cross-section 12.7 mm by 3.2 mm. Specimens to be tested at high and low temperatures were milled from injection-moulded 3.2 mm plates with a 37 mm parallel gauge length and a gauge width of 7 mm. All specimens were annealed at approximately 353 K for 2 h before testing.

2.2. Procedure

Room temperature tensile tests on the three materials were performed on an Instron testing machine using a range of testing rates. Cross-head speeds used ranged from 0.5 to 500 mm min^{-1}. Considering the machine hard with respect to the specimens, the strain-rate was calculated directly from the cross-head speed and the specimen gauge length giving a range of strain-rates from 10^{-4} to 10^{-1} sec^{-1}. A heating chamber was fitted to the Instron to allow tests to be conducted at 333 K. Low temperature tests at 193 K were conducted on a tensile machine fitted with a cryostat: test specimens were enclosed in a vacuum flask, low temperatures being achieved by the controlled boil off of liquid nitrogen. Longi-

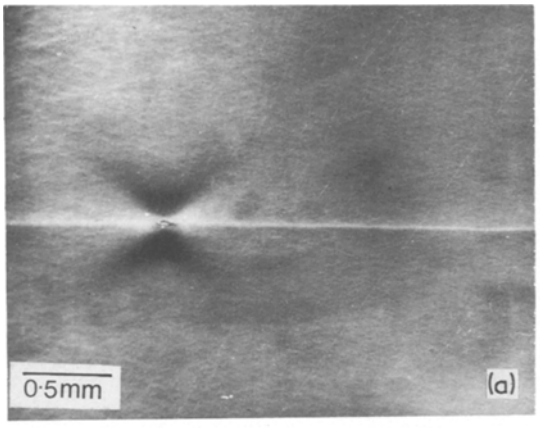

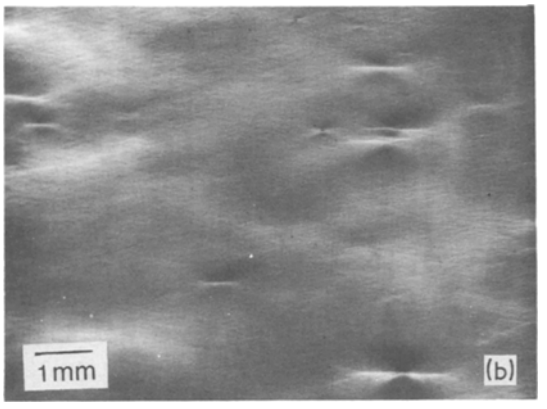

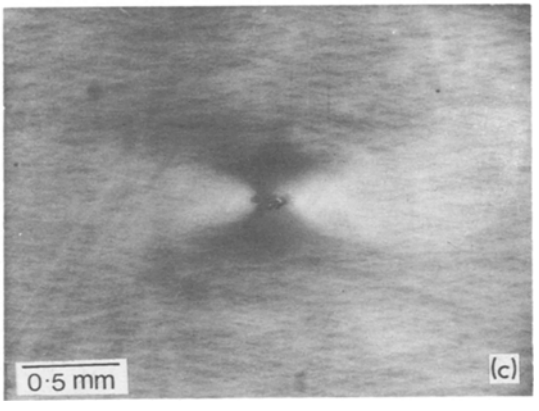

Figure 1 Stress whitening in material C at varying strain-rates: (a) 1.3×10^{-4} sec^{-1}, (b) 1.4×10^{-2} sec^{-1}, (c) 1.4×10^{-1} sec^{-1}. Small cracks can be seen as the first stage of fracture.

tudinal sections were examined with an optical microscope and the fracture surfaces, after coating with aluminium, in the scanning electron microscope.

3. Results

3.1. Observations on longitudinal sections

The variations in stress whitening with strain-rate were similar in each of the three materials having different rubber contents and have been described in detail previously [1, 2]. At a strain-rate of 1.4×10^{-4} sec^{-1}, large distinct planar crazes formed associated with oblique zones of stress whitening which consisted of large numbers of small non-planar crazes. With increasing strain-rate, the planar crazes became smaller and the oblique zones more pronounced until at the highest strain-rate used (1.4×10^{-1} sec^{-1}), a huge number of small crazes clouded the whole gauge length.

Optical micrographs of cracks opening in the high rubber content material C at different strain-rates are shown in Fig. 1. At a strain-rate of 1.4×10^{-4} sec^{-1} (Fig. 1a), a crack can be seen opening up within a large craze. Fanning out from the crack at approximately 45° are regions of highly stress whitened material. At the higher strain-rate of 1.4×10^{-2} sec^{-1} (Fig. 1b), a crack had again nucleated within a distinct craze. At the highest strain-rate used of 1.4×10^{-1} sec^{-1}, surface cracks were observed to nucleate in regions of high stress whitening (Fig. 1c).

Fig. 2 shows a large crack on the surface of a highly strained bar of material C tested at 1.4×10^{-4} sec^{-1}. This crack was approximately 1 mm

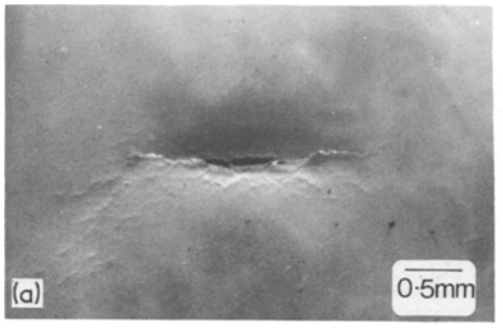

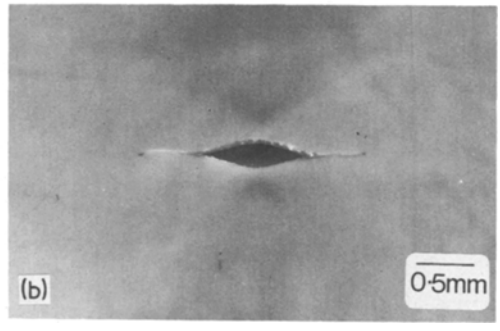

Figure 2 (a) A large crack in the surface of material C tested at 1.4×10^{-4} sec^{-1} (b) serial section.

long and close to the stage of catastrophic propagation. Surrounding this crack was an irregular array of smaller cracks which appear to be strings of voids that have opened up and coalesced in a similar manner to those observed in transparent ABS as reported in an earlier paper [1]. Serial sectioning of the region containing the large crack revealed a large lenticular cavity just below the surface (Fig. 2b). Although the ABS material was severely cold-drawn ($\sim 40\%$ elongation) and totally stress whitened, there appeared to be a feature developing perpendicular to the stress axis ahead of the crack having characteristics similar to those of a craze.

3.2. Fracture surface observations

The appearance of the fracture surface varied little with variations in strain-rate and rubber content in these materials. The site of fracture initiation was clearly identifiable in all samples and ranged from a surface flaw (Fig. 3a), to the more common case of an inclusion within the material (Fig. 3b). These inclusions varied in size from roughly 25 to 300 μm. In general, two distinct regions were observed on the fracture surface and these have been labelled as stage I and stage II in Fig. 3.

3.2.1. Stage I

The initiation site was always the focus of a double cone region on the surface which was associated with slow crack growth. Fine markings radiated out from the initiation site perpendicular to the crack front, appearing to result from the crack propagating on slightly displaced fracture planes. These radial markings are similar to, but do not necessarily correspond with, the river lines observed in large crazes in transparent ABS [1]. Superimposed on the radial markings were secondary fracture parabolas: corresponding areas from opposite fracture surfaces revealed either depressions or protrusions larger than the thickness of a craze centred on these parabolas. A small inclusion was often present at the focus of the parabola. These secondary fracture parabolas resulted from the main fracture front intersecting secondary cracks initiated ahead of and on a neighbouring plane to the main crack front. They were numerous in the lower rubber content materials but were often absent in the high rubber content material.

In some samples, multiple double cone regions appeared on the fracture surface. With the lowest strain-rate used (1.4×10^{-4} sec^{-1}) and the high rubber content material C, several of these cone regions covered almost the entire fracture surface.

The morphology of stage I observed at higher magnification showed little variation among the samples and a typical example (material B tested at 1.4×10^{-3} sec^{-1}) is shown in Fig. 4. It shows that this region of the surface was highly drawn, the drawn fibres being oriented slightly in the direction of crack propagation. This structure was similar to the dimples observed on the fracture surface of metals that have failed in a ductile

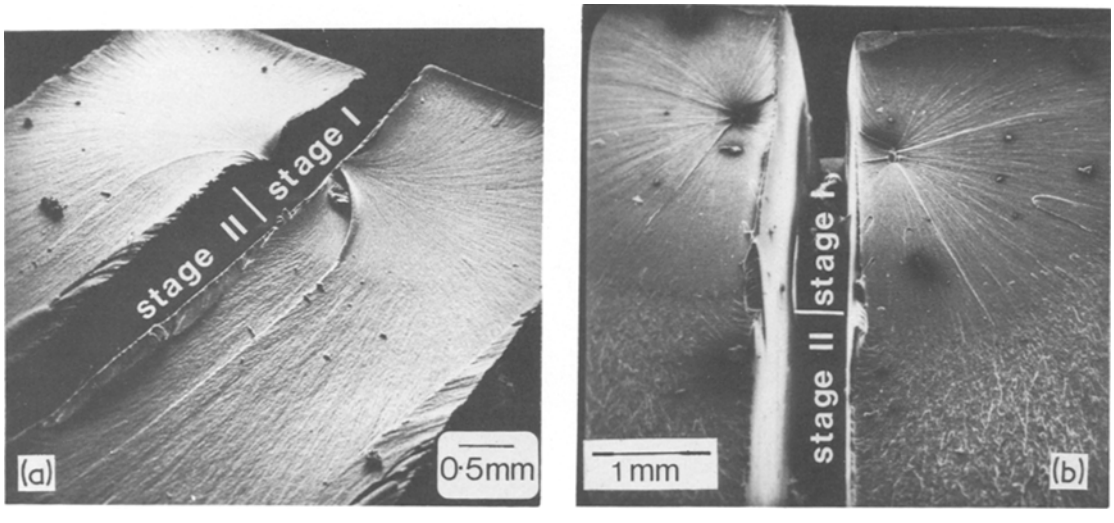

Figure 3 Typical low magnification micrographs of the fracture surfaces of these materials. (a) Material C, strain-rate 1.4×10^{-1} sec^{-1}. (b) Material B, strain-rate 1.4×10^{-3} sec^{-1}.

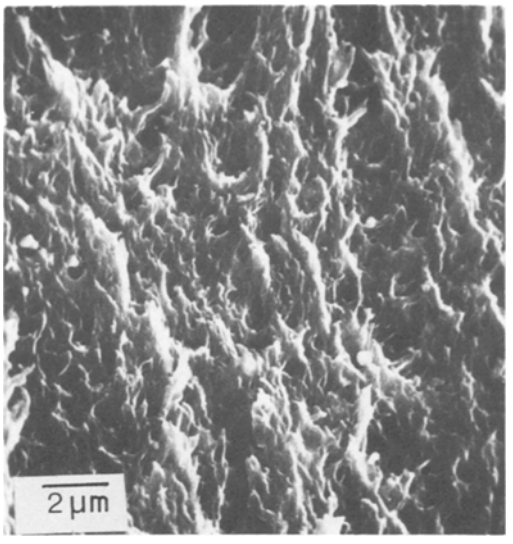

Figure 4 Highly drawn structure of the slow crack propagation region of the fracture surface (material B: strain-rate 1.4×10^{-3} sec^{-1}).

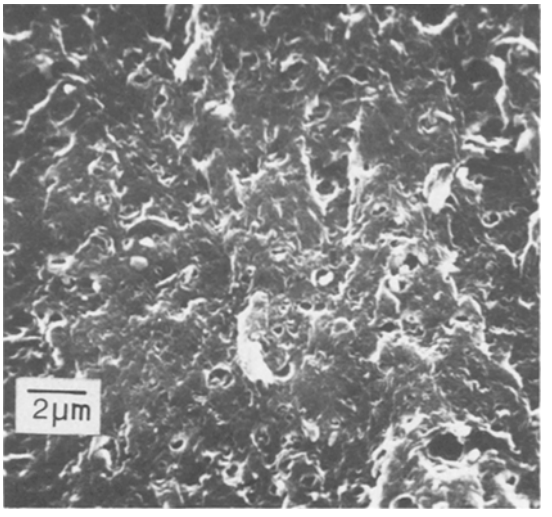

Figure 5 Slow crack propagation region of material. A (strain-rate 1.4×10^{-3} sec^{-1}) viewed almost directly down onto the surface.

fashion. Fig. 5 is a micrograph of the low rubber content material viewed vertically in which the dimples were clearly evident and in some cases particles can be seen within the dimples. The dimples were approximately 0.3 μm in size, the average rubber particle size in the material. They were more numerous in the high rubber content material but the particles were much less distinct in this material.

3.2.2. Stage II

Catastrophic crack growth produced a change in the fracture surface morphology. Features appeared to be more rounded and the crack had stepped between planes in a highly irregular fashion (Fig. 6). This stepping between planes produced the apparent roughness of this region at low magnifications (Fig. 3). The dimple structure was again observed but the drawing of the polymer was less than in the slow crack propagation region. Particles similar to those seen on stage I of the fracture surface were scattered over the surface or were lying in the dimples. These particles were numerous in the low rubber content materials but were again less prominent in the high rubber content material.

The transition from the slow crack growth region to the catastrophic crack growth region was quite distinct at all strain-rates, although at high strain-rates the markings radiating from the crack initiation point gave the appearance of continuing

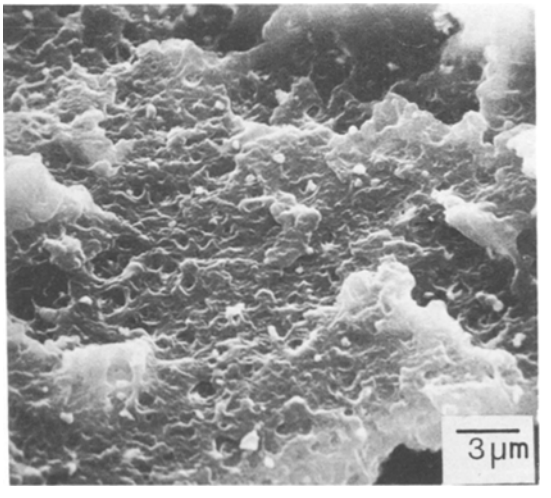

Figure 6 Structure of the fracture surface where the crack was propagating catastrophically (material A: strain-rate 1.4×10^{-1} sec^{-1}).

into the fast crack growth region (Fig. 3a). This apparent continuation of the radial markings into the fast crack growth region was also observed in the high rubber content material at lower strain-rates. However, the change observed at higher magnification in the morphology of the fracture surface from the highly drawn slow crack growth region to the more rounded fast crack growth region was still present under these conditions.

3.3. Effect of temperature

The variation in stress whitening with strain-rate observed at room temperature was maintained in

the lower rubber content materials A and B at 333 K. However, in the high rubber content material C at slow strain-rates, little stress whitening was observed and the material deformed by forming a neck which propagated along the gauge length. Tests at 193 K were conducted only on material B and at this temperature, which is nearing the glass transition temperature of the rubber particles, stress whitening was less evident but there appeared to be a general clouding of the gauge length with no distinct crazes readily observable.

Increasing the temperature from room temperature to 333 K had little effect on the macroscopic fracture surface and this was the case even in the high rubber content material at low strain-rates where the stress whitening decreased. Examination of all the samples at higher magnification revealed that the fracture surfaces within the double cone stage I regions exhibited a considerably greater degree of drawing than at room temperature. Features of the fast crack propagation stage II region tended to be more rounded than at room temperature.

The two stage fracture mechanism was maintained down to 193 K, though at this temperature the slow crack growth region was smaller than at room temperature. Fig. 7 shows that at this temperature there was a tendency for the final fracture plane to deviate from the perpendicular to the applied tensile stress. On several samples, it appeared to be approximately 25° to the normal plane. Higher magnification indicated that a small amount of drawing had still occurred during slow crack growth (Fig. 8). However, the surface of the fast propagation stage II region was a sponge-like void structure which displayed little evidence that drawing of the polymer had taken place (Fig. 9).

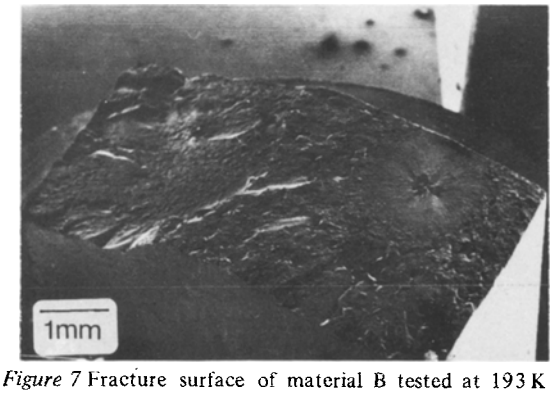

Figure 7 Fracture surface of material B tested at 193 K and strain-rate 10^{-2} sec^{-1}.

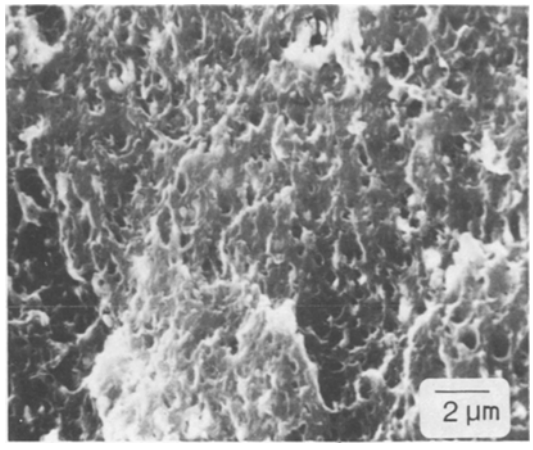

Figure 8 Slow crack propagation region of material B tested at 193 K and strain-rate 10^{-2} sec^{-1}.

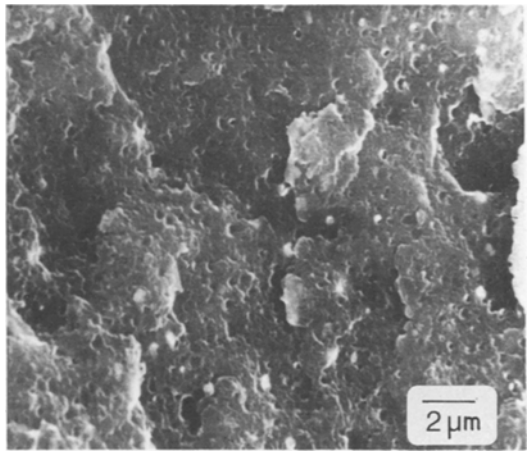

Figure 9 Catastrophic failure region of material B tested at 193 K and strain-rate 10^{-2} sec^{-1}.

4. Discussion

The research reported in this paper gives significant insights into the fracture mechanisms in ABS but several aspects are still unclear. It has been shown that cracks can initiate in crazes but it has not been shown unequivocally that these cracks within crazes lead to the final failure of the specimen. It is also left unresolved whether the crazes crack inherently or only as a result of an inclusion at which the craze itself may even have nucleated. In highly stress whitened material resulting from high elongations at low strain-rates, features similar to crazes appeared ahead of the main crack (Fig. 2b) but the nature of the deformation in this "craze" has not yet been elucidated. Many large crazes formed near the yield point in this particular specimen but it was impossible to locate them at

high elongations due to the heavy stress whitening. The crack may have opened up within one of these crazes or the feature at the crack tip may form at a later stage of the deformation.

However, several major aspects of the fracture processes of ABS have been elucidated by the present observations. In particular, a two-stage fracture process has been resolved and the general features of these two stages have been interpreted.

Final fracture always initiated at an inclusion or a surface defect. Many particles capable of initiating fracture appeared to be present in these materials. Not only was fracture often initiated at inclusions but many samples also displayed secondary fracture parabolas centred on further impurities. The elongation to failure varied considerably among specimens tested under the same conditions of strain rate and temperature. Premature failure in general could be traced to a large inclusion within the material or to a large surface defect while higher elongations occurred when the flaw size was smaller. All of these inclusions were not identified but electron microprobe analysis of one large particle revealed that it had a high calcium content.

The crack initiated at a flaw opened up to a double convex cavity which may have a planar feature ahead of it. The surfaces of this double convex crack corresponded to the stage I cone regions of the fracture surface. The morphology of the stage I region was similar in all materials under differing conditions of strain-rate and temperature. The matrix was highly drawn around rubber particles giving a dimple structure. The number of these dimples increased with increasing rubber content.

At some critical point, the slowly growing crack became unstable and propagated rapidly across the specimen. The fracture surface in this stage II region was more irregular as the crack stepped between planes. Variations in the morphology of this region with strain-rate, and rubber content appeared to correspond with the difference in the crazing characteristics with these parameters. When intense stress whitening occurred at high strain-rate or high rubber content, the morphology was more regular than under conditions where fewer larger crazes formed. The general rounding of the features in the fast crack growth region may have been due in part to polymer annealing due to adiabatic heating. The phenomenon would be expected to be more pronounced at elevated temperatures where in fact evidence for the collapsing of the drawn polymer structure was observed.

5. Conclusions

Fracture in pigmented ABS materials always initiated at a surface defect or at an internal impurity particle. Despite the variation in stress whitening behaviour in the temperature range from 193 to 333 K and in the strain-rate range from 10^{-4} to 10^{-1} sec^{-1}, under all conditions failure occurred by similar mechanisms indicating that initial crazing may not be overwhelmingly important to the fracture processes. A lenticular crack opened at the impurity particle and grew slowly to produce a highly drawn double cone region on the fracture surface. At some critical point, this crack propagated catastrophically producing a more irregular fracture surface as the crack stepped between planes.

Increasing the rubber content of the material had little effect on the macroscopic fracture surface but on a microscopic level, the increased volume of rubber particles provided more sites at which voiding and drawing of the polymer could occur.

Increasing the temperature from 193 to 333 K also had little effect on a macroscopic level but on a microscopic level increased the degree of drawing on the fracture surface.

Acknowledgements

The polymeric material on which this research was conducted was generously provided by Marbon Chemical (Australia) Pty Ltd. R.W.T. is grateful for the provision of a Commonwealth Postgraduate Research award.

References

1. R. W. TRUSS and G. A. CHADWICK, *J. Mater. Sci.* **11** (1976) 1385.
2. *Idem, ibid* **11** (1976) 111.

Received 26 May and accepted 25 June 1976.